Numerical simulation of a single molten 316SS droplet penetrating into sodium pool with MPS method

YANG Zhi[1], ZHANG Zhi-gang[2,*], WEI Wei[3], and HAO Xiao-yu[4]

1. Fundamental Science on Nuclear Safety and Simulation Technology Laboratory, Harbin Engineering University, Number 145, Nantong Street, Harbin 150001, China (yang_zhi@hrbeu.edu.cn)
2. Fundamental Science on Nuclear Safety and Simulation Technology Laboratory, Harbin Engineering University, Number 145, Nantong Street, Harbin 150001, China (zg_zhang@hrbeu.edu.cn)
3. Fundamental Science on Nuclear Safety and Simulation Technology Laboratory, Harbin Engineering University, Number 145, Nantong Street, Harbin 150001, China (wei1993126@163.com)
4. Fundamental Science on Nuclear Safety and Simulation Technology Laboratory, Harbin Engineering University, Number 145, Nantong Street, Harbin 150001, China (haoxiaoyu@hrbeu.edu.cn)

Abstract: Severe core disruptive accidents in the sodium-cooled fast reactor and core molten materials and the coolant sodium interaction (including fuel-coolant interaction and structural material-coolant interaction), are one of the international key and difficult problems on the core safety studies of reactor, especially for drastic changes of the multiphase flow, heat transfer between cold and hot molten fluid interface, deformation and fragmentation behaviors of the molten material, *etc*. Considering that there are so many difficulties with large deformation and numerical diffusion problems in traditional mesh method, a meshless moving particle semi-implicit (MPS) method is introduced to the present structural material-coolant interaction research. The viscosity model, surface tension and passively moving solids (PMS) model are all taken into consideration. With the improved MPS algorithm, the stability and accuracy of the computation have much increased. The present MPS method is validated by simulating the experiments of a single molten Type 316 stainless steel (316SS) droplet penetrating into sodium pool which was conducted by Zhang. The penetrating, fragmentation and solidification process of the droplet in the simulation are discussed. The comparison of the predicted dimensionless fragment size (D / D_0) distribution with the experimental results shows a good agreement for the small-sized fragments part. The present research indicates that the typical solidification and fragmentation behavior of the structural material-coolant interaction process can be successfully simulated by MPS method.
Keyword: structural material-coolant interaction; molten 316SS droplet; MPS method; solidification; fragmentation

1 Introduction

For the termination of severe core disruptive accidents (CDAs) in metallic fuel fast breeder reactors (FBRs), the molten core materials are required to be passively discharged from the core region and cooled down in the lower plenum. Therefore, it is necessary to fully investigate the possibility and mechanism of thermal fragmentation and hydrodynamic fragmentation due to molten core material–sodium coolant interaction.

From this point of view, a series of experiments about a single molten metal droplet penetrating sodium pool were conducted by Zhang [1]. Molten stainless steel and copper were chosen as the molten material simulant, and the experiments were conducted in relatively wide ranges of thermal and hydrodynamic conditions. Empirical equations for the fragment size distributions with respect to We_a and T_i were developed. The result demonstrated that intensive fragmentation is much more likely to be observed with a higher We_a at $T_i << T_{ss,mp}$. The fragment sizes with a higher We_a are somewhat less than those with the lower We_a under the same thermal conditions.

Though experiments may be the most direct way to learn about molten material fragmentation in FBRs, the experimental conditions are limited considering that the experiments require a large amount of time and cost. Thus it is necessary to carry out numerical simulations. However, considering that

Received date: January 24, 2017
(Revised date: March 14, 2017)

there are so many difficulties with large deformation and numerical diffusion problems in traditional mesh method for molten material fragmentation research, a meshless moving particle semi-implicit (MPS) method based on a fully Lagrangian description is introduced to this research [2]. Numerical diffusion doesn't arise because convention terms are not discretized. MPS method has been verified to be effective for many applications, especially for thermal-hydraulic problems with free surface and two-phase flow problems with a moving interface. It has been successfully applied to various research areas to deal with the free surface flow and large deformation. The MPS method was first applied to solid-liquid two-phase flow of breaking waves with a passively moving float through a model of a passively moving solid (PMS) [3]. With the surface tension model based on potential method, the MPS method was also applied to gas-liquid two-phase flow analysis of void distribution in a circular tube and two-fluid flow analysis of water jet into a gasoline pool [4,5]. With the viscosity model and the improved surface tension model, the solidification and melting behaviors of the melt materials were simulated precisely and the results were consistent with the experiments [6,7]. Jet injection behavior for fuel-coolant interactions (FCI) without calculating the energy equation and numerical simulation of molten core-concrete interactions (CCI) were investigated [8,9].

Considering that numerical simulation usually became unstable when the fluid particles impacted on the wall with relatively large velocity in the origin MPS method, the essential theory of the finite volume particle (FVP) [10,11], a newly developed particle method, was introduced into the present MPS method. There was no special treatment for the particles on the free surface, and it was not necessary to find out the particles on the free surface on each time step correspondingly. Thus the stability of simulation was improved.

In the present research, the improved MPS method, which combined the existing viscosity model, surface tension model, PMS model with the FVP method, is firstly applied to simulate the experiments conducted by Zhang of a single molten 316SS droplet penetrating into the sodium pool, which involved liquid-solid two-phase flow and phase change [1]. The penetrating, fragmentation and solidification process of the simulation are discussed. The results of dimensionless fragment size (D/D_0) distribution and the dimensionless mass median diameter (D_m/D_0) were then compared with the experimental results.

2 Numerical method

2.1 Governing equations

The governing equations include the mass, momentum and energy conservation equations.

$$\nabla \cdot \mathbf{u} = 0 \tag{1}$$

$$\frac{D\mathbf{u}}{Dt} = -\frac{1}{\rho}\nabla P + \nu \cdot \nabla^2 \mathbf{u} + \mathbf{f} \tag{2}$$

$$\frac{D(\rho h)}{Dt} = \nabla \cdot (k\nabla T) + Q \tag{3}$$

Where $t, \rho, \mathbf{u}, P, \nu, \mathbf{f}, h, k, T$ and Q are time, fluid density, velocity vector, pressure, kinetic viscosity, external force, enthalpy, thermal conductivity, temperature and heat source term respectively.

2.2 Particle interaction models

The key idea of MPS method is discretizing the fluid into a series of particles and developing a set of particles interaction models. Among these particle interaction models, the most important one is the kernel function. Actually, it is a weight function. The physical quantity of the particle can be evaluated from the quantity of the particles surrounding it. The kernel function used in this paper is as follows:

$$w_{ij} = w(|\mathbf{r}_{ij}|) = \begin{cases} \dfrac{R_e}{|\mathbf{r}_{ij}|} - 1 & |\mathbf{r}_{ij}| \le R_e \\ 0 & |\mathbf{r}_{ij}| > R_e \end{cases} \tag{4}$$

$$\mathbf{r}_{ij} = \mathbf{r}_j - \mathbf{r}_i \tag{5}$$

Where R_e is the cutoff radius used for limiting the interactions. In the present MPS method, it is chosen to be $3.2\,l_0$ to ensure the precision of the calculation, where l_0 is the initial distance between two particles. $|\mathbf{r}_{ij}|$ is the distance between two particles *i* and *j*. Particle number density of particle *i* is the summation of weight function just as is shown in Eq(6).

$$n_i = \sum_{j \ne i} w(|\mathbf{r}_j - \mathbf{r}_i|) \tag{6}$$

To obtain more stable numerical simulations, the discretization form of the gradient and Laplacian operators are expressed as follows, which are widely used in the FVP method.

$$\langle \nabla \phi \rangle_i = \frac{S}{n_0 V} \sum_{j \neq i} (\phi_i + \frac{\phi_j - \phi_i}{|\mathbf{r}_{ij}|}) w_{ij} \mathbf{n}_{ij} \tag{7}$$

$$\langle \nabla^2 \phi \rangle_i = \frac{S}{n_0 V} \sum_{j \neq i} \frac{\phi_j - \phi_i}{|\mathbf{r}_{ij}|} w_{ij} \tag{8}$$

$$\mathbf{n}_{ij} = \frac{\mathbf{r}_j - \mathbf{r}_i}{|\mathbf{r}_{ij}|} \tag{9}$$

Where S and V are the area and the volume of a single particle respectively. S and V are equivalent to $2\pi R$ and πR^2 in the two-dimensional system, where R is $l_0/\sqrt{\pi}$. n_0 is the initial particle number density, which is calculated at the beginning of the entire simulation. $\mathbf{n}_{ij}$ is the unit vector.

2.3 Surface tension model

It is necessary to estimate the surface tension for the liquid phase during the melting and solidification process. Surface tension model based on the potential force between particles is introduced to this research as it is well suited to the particle method [12]. As is shown in Eq(10), the potential force is repulsive when $r < l_0$ and attractive when $l_0 < r < R_e$.

$$f = C \cdot (r - l_0) \cdot (r - R_e) / m \tag{10}$$

Where C is a fitting coefficient and m is the mass of a single particle. The potential force coefficient between fluid particles is given as follows.

$$C = \frac{2\sigma l_0^2}{\sum_{i \in A,\, j \in B,\, |\mathbf{r}_{ij}| < R_e} \frac{1}{3}(r - \frac{3}{2} l_0 + \frac{1}{2} R_e)(r - R_e)^2} \tag{11}$$

Where σ is the surface tension coefficient of the molten stainless steel.

2.4 Viscosity model

As the latent heat releases, the viscosity of the droplet particles increases significantly and it has a great impact on the penetration behavior. In a previous research on the viscosity models for corium melts, Ramacciotti *et al* developed an empirical correlation in which the viscosity of the melts changed in the exponential form [13]. Thus in the present research, the similar form is adopted to evaluate the viscosity of the droplet particles in the phase transition state.

$$\nu = \nu_l \cdot e^{K(1-\alpha)} \tag{12}$$

Where ν_l is the viscosity of stainless steel in liquid phase. K is a coefficient and is chosen to be 5 in this paper. α is the liquid phase volume fraction, and is defined as follows.

$$\alpha = \begin{cases} 0 & h < h_s \\ \dfrac{h - h_s}{h_l - h_s} = \dfrac{h - h_s}{L} & h_s < h < h_l \\ 1 & h_l < h \end{cases} \tag{13}$$

Where h_l and h_s are the enthalpy in liquid phase and in solid phase at the melting point respectively. h is the enthalpy of the particle and L is the latent heat. Figure 1 shows the detailed relationship between T, α, and h.

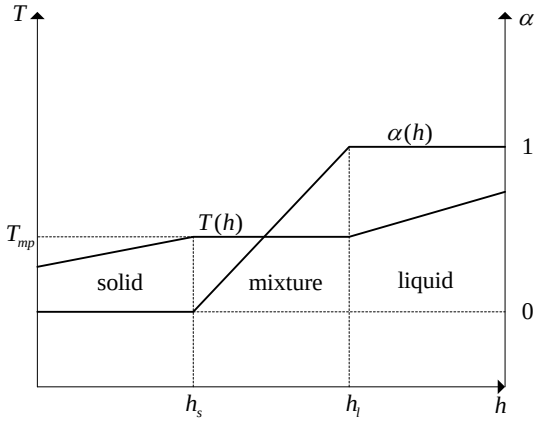

Fig.1 Relationship between T, α and h.

2.5 PMS model

During the penetration process, the droplet breaks up and generates many fragments. In this paper, we put forward a fragment judgment criterion. A stainless steel particle i and particle j are considered to be in one fragment if they satisfy the following two requirements. Firstly, particle i and particle j should in the phase transition state. Secondly, the distance between them should satisfy $|\mathbf{r}_{ij}| \leq \varepsilon \cdot l_0$, where ε is a coefficient. Both too small and too large coefficient will lead to inaccurate results. ε is evaluated to be 1.2 in this paper. As the fragment composition is clear, the movement of the fragment is calculated, according to the passively moving solid (PMS) method [3].

2.6 Algorithm

A semi-implicit algorithm is used in the original MPS method, in which the viscosity and the external force terms in the momentum conservation equation were explicitly calculated in each time step [2]. However,

the viscosity of the droplet changes with respect to the liquid phase volume fraction in the structural material-coolant interaction process. In this situation, the process cannot be effectively simulated using the original MPS method [7]. To overcome this problem, an implicit calculation of viscosity term is recommended in this research. Figure 2 shows the detail calculation procedure of the present MPS method. In each time step, the particle temperature is updated according to the particle enthalpy by explicitly calculating the diffusion term of energy equation with boundary condition as following equations.

$$h^{n+1} = h^n + \Delta t \cdot \frac{k}{\rho} \nabla^2 T^n \tag{14}$$

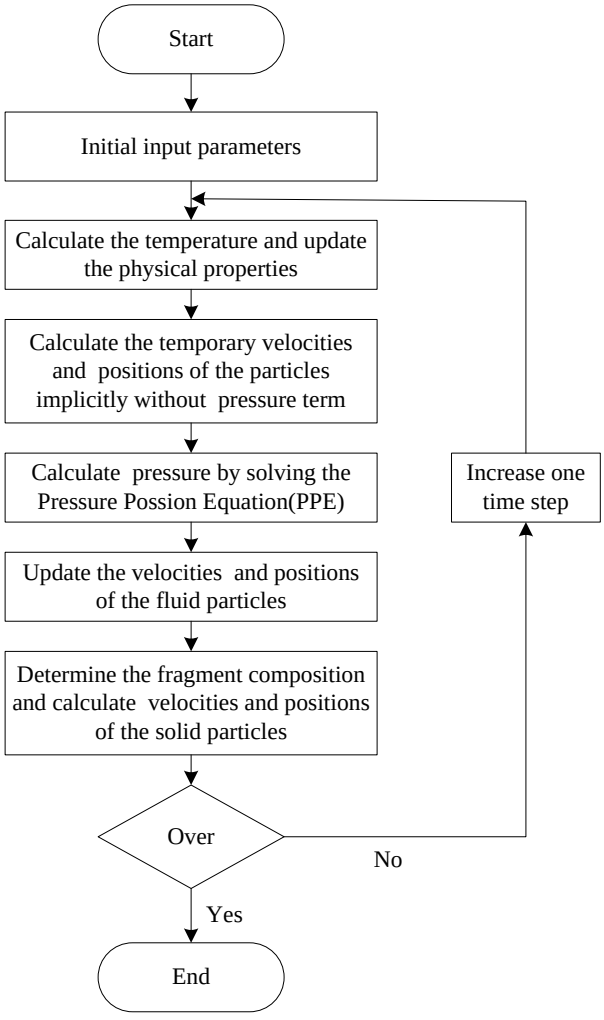

Fig.2 Algorithm of the present MPS method.

Then the density and viscosity of the droplet particles are updated based on the liquid phase volume fraction. To overcome the numerical difficulties arising from large differences in density and viscosity between liquid and solid phases, the density and viscosity of particle *i* are then smoothed using the following equations [10].

$$\rho_i = \frac{\sum_{j \in R_e} \rho_j \cdot w_{ij}}{\sum_{j \in R_e} w_{ij}} \tag{15}$$

$$\nu_i = \frac{\sum_{j \in R_e} \nu_j \cdot w_{ij}}{\sum_{j \in R_e} w_{ij}} \tag{16}$$

Next, the viscosity term and the surface tension term in Eq(2) are implicitly calculated without the pressure gradient term, and the temporary velocity $\mathbf{u}_i^*$ and temporary position $\mathbf{r}_i^*$ are obtained.

$$\mathbf{u}_i^* - \nu \Delta t \cdot \nabla^2 \mathbf{u}_i^* = \mathbf{u}_i^n + \Delta t \cdot \mathbf{f} \tag{17}$$

$$\mathbf{r}_i^* = \mathbf{r}_i^n + \Delta t \cdot \mathbf{u}_i^* \tag{18}$$

Where the superscript *n* and * denote the time step in calculation and the temporary sub-step in one time step. Then the pressure of the particles can be calculated by solving the Pressure Poisson Equation.

$$\nabla^2 P_i^{n+1} = \frac{\rho}{\Delta t} \nabla \cdot \mathbf{u}_i^* \tag{19}$$

At last, the final velocity $\mathbf{u}_i^{n+1}$ and position $\mathbf{r}_i^{n+1}$ are updated.

$$\mathbf{u}_i^{n+1} = \mathbf{u}_i^* - \frac{\Delta t}{\rho} \nabla P_i^{n+1} \tag{20}$$

$$\mathbf{r}_i^{n+1} = \mathbf{r}_i^n + \Delta t \cdot \mathbf{u}_i^{n+1} \tag{21}$$

3 Numerical simulation

3.1 Experiments on single molten 316SS droplet penetrating a sodium pool

A series experimental study on fragmentation of a single molten metal droplet penetrating a sodium pool was conducted by Zhang [1]. 316SS is now the material most commonly used for cladding and assembly ducts in FBRs because of its good high temperature properties, its resistance to swelling, and its high corrosion-resistant properties. Thus in this study, two cases of the experiments on a single 316SS droplet penetrating a sodium pool were simulated and the experimental conditions and results are listed in Table 1. T_i, which is the instantaneous contact interface temperature between a single molten droplet and the liquid sodium, is theoretically calculated as a one-dimensional heat conduction problem in semi-infinite geometry, and T_i is calculated as is shown in Eq(22).

$$T_i = \frac{\sqrt{\lambda_c \rho_c C_{pc}} T_c + \sqrt{\lambda_h \rho_h C_{ph}} T_h}{\sqrt{\lambda_c \rho_c C_{pc}} + \sqrt{\lambda_h \rho_h C_{ph}}} \tag{22}$$

Where λ_c , λ_h , ρ_c , ρ_h , C_{pc} and C_{ph} are thermal conductivity of the sodium and the droplet, the density of the sodium and the droplet and the specific heat of the sodium and the droplet. We_a, which is the ambient Webber number, is proportional to the ratio of the disruptive hydrodynamic force to the stabilizing surface tension, and the definition of We_a is given in Eq(23).

$$We_a = \frac{\rho_c V_0^2 D_0}{\sigma} \tag{23}$$

Where V_0 and D_0 are the initial velocity and initial diameter of the droplet. According to the previous experimental research about a single stainless steel droplet penetrating into the sodium pool, T_i and We_a can perfectly represent the thermal and hydrodynamic conditions respectively [1]. Thus the following analysis are based on these two parameters.

3.2 Computation domains

In the present research, a two-dimensional calculation geometry is adopted as is shown in Figure 3, considering the symmetrical characteristic of the simulation, as well as the limitation of the complexity of the three-dimensional geometry. The droplet, with the diameter of approximate 11.3mm, is represented by 400 stainless steel particles. In the initial arrangement of the particles, the droplet is placed just above the sodium pool surface with an initial velocity, skipping the acceleration process when the droplet declines in the air. The sodium pool is represented by 40000 particles with the size of $100\text{mm}\times100\text{mm}$. In the present research, four layers of solid wall are adopted. To get more precise results, smaller l_0 should be adopted. In the present research, l_0 is set to be 0.5mm, and correspondingly a smaller time step Δt of $2\mu s$ is adopted. The present simulations exclude the heat transfer from the droplet and the wall to the surrounding air because its effect on fragmentation and solidification is negligibly small over the short time period.

The thermophysical and physical properties of 316SS and liquid sodium in the simulation are listed in Table 2. The simulation conditions and results are listed in Table 3.

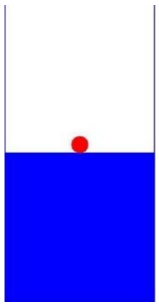

Fig.3 Computation domains of structural material-coolant interaction simulation.

Table 1 Experimental conditions and results

	Melt	Melt temperature T_h (℃)	Sodium temperature T_c (℃)	Instantaneous contact Interface temperature T_i (℃)	Initial diameter of the droplet D_0 (mm)	We_a	Mass median diameter D_m (mm)	D_m/D_0
Case1	316SS	1510	299	915	11.5	90	5.69	0.49
Case2	316SS	1564	309	949	15.8	123	5.01	0.32

Table 2 Thermophysical and physical property of stainless steel and sodium

Thermophysical and Physical Property	316SS		Na[b]
	Solid	Liquid[a]	
Melting point(℃)	1427		98
Density (kg/m^3)	7954	6920	880
Specific heat (KJ/Kg.K^{-1})	0.502	0.775	1.345
Thermal conductivity (W/m.K^{-1})	13.96	18.30	77.0
Thermal diffusivity (mm^2/s)	3.50	3.41	64.98
Latent heat (KJ/Kg)	270		—
Kinetic viscosity (mm^2/s)	—	0.775	0.397
Surface tension (mN/m)	—	1830	177

a. values at superheat degree of 100℃.

b. values at temperature of 300℃.

Table 3 Simulation conditions and results

	Melt	Melt temperature T_h (℃)	Sodium temperature T_c (℃)	Instantaneous contact interface temperature T_i (℃)	Initial diameter of the droplet D_0 (mm)	Initial velocity of the droplet V_0 (m/s)	We_a	Mass median diameter D_m (mm)	D_m/D_0
Case1	316SS	1510	299	915	11.3	4.07	90	4.73	0.44
Case2	316SS	1564	309	949	11.3	4.76	123	4.05	0.36

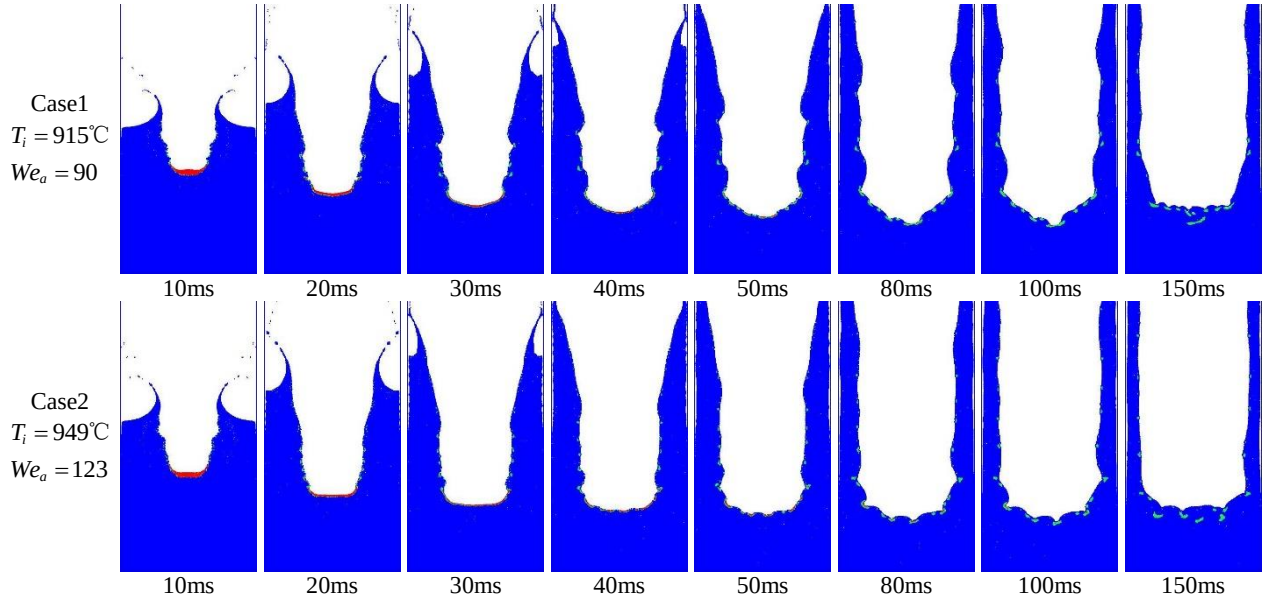

Fig.4 The simulation of penetrating, fragmentation and solidification process.

The initial temperature of 316SS and sodium pool in the simulations are set to be identical to the experimental conditions. The same droplet diameter of 11.3mm is adopted in the simulations for convenience, and the initial velocities of the droplet are calculated to keep the We_a numbers same as those in the experiments.

3.3 Penetrating process

Figure 4 shows the simulation of the penetrating, fragmentation and solidification process of a single molten 316SS droplet. In Fig.4 different colors are used to distinguish different material and state. The sodium particles are represented by blue color, and the molten state of 316SS particles are represented by red color and change to green color when the 316SS particles solidify. Drastic fragmentation of the droplet is observed and there is some sodium splashing out of the pool in both two cases because of the relatively high We_a number.

For the condition with T_i value of 915℃ and We_a number of 90 in case 1, it is clearly found that the droplet deforms to be an oval shape (10ms) due to the inertia of the droplet and the hydrodynamic resistance of the sodium when the molten droplet penetrates into the sodium pool. Meanwhile the sodium is pushed to the sides of the pool because of the impact of the droplet, and gets the upward velocity. Then a flat leading edge is formed at the bottom surface of the molten droplet (20ms), and there are some small fragments stripping off the droplet (30ms). Then the leading edge becomes longer and longer (40ms) and at last fragments due to the drag force (50ms). The fragments generated then solidify. At last the sodium pushed up falls to the pool again. In case 1, the droplet fragments into several large-sized fragments and many small-sized fragments.

Compared with the case 1, case 2 shows the structural material-coolant interaction process with higher T_i value of 949℃ and We_a number of 123. Much more fragments are generated and there is more sodium splashing out of the pool. It is the same as in case 1 except for deeper penetration distance at the beginning (10ms). There is also a flat leading edge at the bottom of the droplet (20ms). Then the center of the edge becomes curved and two sides of

the edge becomes longer and longer with many small fragments detaching from the droplet (30ms). Then, the leading edge starts to deform and split into a lot of fragments (40ms), which is faster than that in case 1. At last the sodium pushed up falls to the pool. With the impact of the sodium, the edge deforms further and fragments. In case 2 of higher T_i value and We_a number, the droplet fragments drastically, and there are several medium-sized fragments and many small-sized fragments.

In the present simulation, when the interface temperature is below the nucleating temperature of the droplet, a thin solid crust is expected to be formed on the bottom surface of the droplet because of the contact with the surrounding sodium. It is expected that the molten metal droplet with an amount of enthalpy and large inertia due to high penetrating velocity can breach the decelerated bottom surface of the thin solid crust and directly enter and make contact with sodium, finely fragmenting.

3.4 Comparison of the simulation and experiment results

To validate the present MPS method for a single molten 316SS droplet penetrating into the sodium pool, the comparison of D/D_0 values between experiments and simulations results are given in Fig.5.

For case 1, D/D_0 distributions for the experiment and the simulation are almost consistent with each other when the cumulative mass fraction is lower than about 0.6, which part consists of small-sized fragments. However, D/D_0 distributions show a great difference when the cumulative mass fraction is over about 0.6, and this can be caused by the errors in modeling the large-sized fragments. However, the overall D/D_0 distribution trend of the simulation agrees with that of the experiment. And D_m/D_0 value, which is a key parameter reflecting the extent the fragmentation, of the simulation is 0.44, which is similar to 0.49 of the experiment. It is notable that the D/D_0 values of some points are greater than 1 in case 1. Actually the fragments generated are mostly of irregular shapes, and in this paper, the fragment size (D) is evaluated to be the length of the longest part of the fragment. For the largest fragment, the D/D_0 value is likely to be greater than 1.

For case 2, the overall D/D_0 distributions trend are similar to that in case 1. D/D_0 distributions in the simulation and the experiment show a great agreement when cumulative mass fraction is less than 0.7, and D/D_0 distributions have a great difference when cumulative mass fraction is over 0.7. Nevertheless, D_m/D_0 of the simulation is 0.36, which is also similar to 0.32 in the experiment.

It is remarkable that D/D_0 distribution curves in case 1 are higher than those in case 2. It indicates that the droplet is fragmented finer, and more and smaller fragments are generated with relatively higher thermal and hydrodynamic conditions.

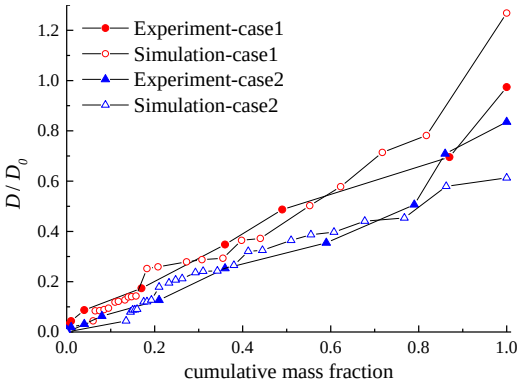

Fig.5 comparison of D/D_0 values between experiments and simulations results.

4 Conclusion

In this research, the improved MPS method was introduced to simulate the structural material-coolant interaction behavior of a single molten 316SS droplet penetrating into sodium pool. The conclusions are summarized as follows:

1. The penetrating, fragmentation and solidification process of the simulation are discussed. At first, the droplet deforms to be an oval shape due to the inertia of the droplet and the hydrodynamic resistance of the sodium. There will be a flat leading edge at the bottom of the droplet. Then the center of the edge becomes curved and two sides of the edge become longer and longer with many small fragments detaching from the droplet. Then, the leading edge starts to deform and splits into a lot of fragments. At last the sodium pushed up will fall to the pool. With the impact of the sodium, the edge deforms further and fragments.

2. The comparison of D/D_0 distributions of the simulations and experiments shows that small-sized fragments are modeled pretty well and there are errors in modeling large-sized fragments in the present simulations. Nevertheless, the key diameter D_m/D_0 of the simulation was similar to that of the experiment. It indicates that the droplet is fragmented finer, and more and smaller fragments are generated with relatively higher thermal and hydrodynamic conditions.
3. With present improved MPS algorithm, both the stability and accuracy of the computation have increased a lot. This demonstrates that the MPS method, with the present effective viscosity model, surface tension model and PMS model, is applicable to simulations of the rheological behavior in complicated multiphase flows with phase-change phenomena. It is also expected that numerical simulations using the present model and MPS method will be useful for detailed analyses of similar phenomena in CDAs.

Acknowledgement

This research was supported by Project of the National Nature Science Foundation of China [grant number 51476040 and 11105034] and Project of Fundamental Research Funds for the Central Universities of China. The authors thank them for the financial support.

References

[1] ZHANG, Zhi-gang: An Experimental Study on Fragmentation of a Single Molten Metal Droplet Penetrating a Sodium Pool, Sapporo: Hokkaido University, 2010.

[2] KOSHIZUKA, S., and OKA, Y.: Moving-Particle Semi-Implicit Method for Fragmentation of Incompressible Fluid, Nucl. Sci. Eng, 1996, 123(3):421-434.

[3] KOSHIZUKA, S., NOBE, A., and OKA, Y.: Numerical Analysis of Breaking Waves Using the Moving Particle Semi-Implicit Method, Int. J. Numer. Meth. Fl, 1998, 26(7):751-769.

[4] SHIRAKAWA, N., HORIE, H., YAMAMOTO, Y., and *et al.*: Analysis of the Void Distribution in a Circular Tube with the Two-Fluid Particle Interacthion Method, J. Nucl. Sci. Technol, 2001, 38(6):392-402.

[5] SHIRAKAWA, N., HORIE, H., YAMAMOTO, Y., and *et al.*: Analysis of Jet Flows with the Two-Fluid Particle Interaction Method, J. Nucl. Sci. Technol, 2001, 38(9):729-738.

[6] LI, G., OKA, Y., and FURUYA, M.: Experimental and Numerical Study of Stratification and Solidification/Melting Behaviors, Nucl. Eng. Des, 2014, 272:109-117.

[7] CHEN, R. H., OKA, Y., LI, G., and *et al.*: Numerical Investigation on Melt Freezing Behavior in a Tube by MPS Method, Nucl. Eng. Des, 2014, 273:440-448.

[8] IKEDA, H., KOSHIZUKA, S., OKA Y., and *et al.*: Numerical Analysis of Jet Injection Behavior for Fuel-Coolant Interaction Using Particle Method, J. Nucl. Sci. Technol, 2001, 38(3):174-182.

[9] LI, X., and OKA, Y.: Numerical Simulation of the SURC-2 and SURC-4 MCCI Experiments by MPS Method, Ann. Nucl. Energy, 2014, 73:46-52.

[10] GUO, L., KAWANO, Y., ZHANG, S., and *et al.*: Numerical Simulation of Rheological Behavior in Melting Metal Using Finite Volume Particle Method, J. Nucl. Sci. Technol, 2010, 47(11):1011-1022.

[11] MAHMUDAH, R.S.N., KUMABE, M., SUZUKI, T., and *et al.*: 3D Simulation of Solid-Melt Mixture Flow with Melt Solidification Using a Finite Volume Particle Method, J. Nucl. Sci. Technol, 2011, 48(10):1300-1312.

[12] KONDO, M., KOSHIZUKA, S., SUZUKI, K., and *et al.*: Surface Tension Model Using Inter-Particle Force in Particle Method, 5th Joint Fluids Engineering Conference, American Society of Mechanical Engineers, 2007:93-98.

[13] RAMACCIOTTI, M., JOURNEAU, C., SUDREAU, F., and *et al.*: Viscosity Models for Corium Melts, Nucl. Eng. Des, 2001, 204(1):377-38.